Multivariable identification of continuous-time fractional system

Magalie Thomassin, Rachid R. Malti

Proceedings of the ASME 2009 International Design Engineering Technical Conferences & Computers and Information in Engineering Conference
IDETC/CIE 2009
August 30-September 2, 2009, San Diego, USA

DETC2009-86975

MULTIVARIABLE IDENTIFICATION OF CONTINUOUS-TIME FRACTIONAL SYSTEM

Magalie Thomassin*, Rachid Malti
Université de Bordeaux, IMS, CNRS UMR 5218
351 cours de la Libération, 33405 Talence Cedex, France
{magalie.thomassin,rachid.malti}@laps.ims-bordeaux.fr

ABSTRACT

This paper presents two subspace-based methods, from the MOESP (MIMO output-error state space) family, for state-space identification of continuous-time fractional commensurate models from sampled input-output data. The methodology used in this paper involves a continuous-time fractional operator allowing to reformulate the problem so that the state-space matrices can be estimated with conventional discrete-time subspace techniques based on QR and singular value decompositions. The first method is a deterministic one whereas the second approach takes place in a stochastic context. The performance of both methods is demonstrated using Monte Carlo simulations at various signal-to-noise ratios. The deterministic method leads, as expected, to biased estimates. This bias is removed in the stochastic method by the use of an instrumental variable. As compared to rational systems, the commensurate differentiation order must be estimated besides the state-space matrices which is done using nonlinear programming. This is the first work developed for multi-input multi-output system identification using fractional models.

1 INTRODUCTION

Fractional models have witnessed a growing interest during the last years. Many diffusive phenomena can be modeled by fractional transfer functions. In electrochemistry for instance, diffusion of charges in acid batteries is governed by Randles models [1] that involve Warburg impedance with an integrator of order 0.5. Electrochemical diffusion showed to have a tight relation with derivatives of order 0.5 [2]. In thermal diffusion of a semi-infinite homogeneous medium, Battaglia *et al.* [3] have shown that the solution for the heat equation links thermal flux to a half order derivative of the surface temperature on which the flux is applied.

Time-domain system identification using fractional models was initiated in the late nineties. Oustaloup [4] developed a method based on the discretization of the fractional differential equation using Grünwald definition and on the estimation of its coefficients using least squares. Trigeassou *et al.* [5] based their identification method on the approximation of a fractional integrator by a rational model. Then, they deduced the fractional model after estimating its rational approximation. Cois *et al.* [6] proposed several extensions of equation error methods, such as the state variable filters and the instrumental variable (IV), to fractional system identification. Aoun *et al.* [7] synthesized fractional orthogonal bases generalizing various bases (Laguerre, Kautz,...) to fractional differentiation orders for identification issues. Recently, Malti *et al.* [8] have extended the concept of optimal IV methods to fractional systems. For an overview of these identification methods refer to [9].

In this paper, we consider the problem of identification of a continuous-time fractional system in its state-space form. Only few papers deal with system identification using fractional state-space representation [6, 10]. They are based on the minimization of an output error criterion by nonlinear programming techniques. These methods are well suited for single-input single-output (SISO) systems, and are generally difficult to apply in the multi-input multi-output (MIMO) case because the number of parameters to estimate becomes large. Here, subspace methods are proposed to estimate the matrices of the continuous-time

*Author to whom correspondance should be addressed.

fractional state-space representation. It is an extension of the methods presented in the literature for rational (thus non fractional) systems [11–13] to the fractional case. Other subspace techniques for identifying continuous-time rational models can be found in [14–17]. So, the proposed method inherits the advantages of subspace methods which stem from the reliability of numerical algorithms using the QR and the singular value decompositions [18]. Thus, it does not involve nonlinear optimization to obtain state-space matrices. In addition, no canonical form (such as modal or companion realizations) of the state-space representation is required. Finally, the proposed subspace algorithms can be applied to the identification of both SISO and MIMO fractional systems. As will be seen later, the state-space representation of a fractional commensurate system involves an additional parameter which is the commensurate order. It is the only parameter computed by minimizing an output error criterion with a nonlinear optimization technique.

In section 2, some recalls about fractional systems are presented. Section 3 presents the methods proposed to estimate the matrices of the continuous-time fractional state-space representation, followed by section 4 devoted to the estimation of the fractional commensurate order using a nonlinear optimization technique. Finally, simulation examples are given in section 5. Monte Carlo simulations are made to show the estimator statistical properties.

2 FRACTIONAL SYSTEMS

A SISO fractional system is governed by a fractional differential equation:

$$y(t)+a_1\mathcal{D}^{\alpha_1}y(t)+\cdots+a_{m_A}\mathcal{D}^{\alpha_{m_A}}y(t)= b_0\mathcal{D}^{\beta_0}u(t)+b_1\mathcal{D}^{\beta_1}u(t)+\cdots+b_{m_B}\mathcal{D}^{\beta_{m_B}}u(t)$$

where $(a_j,b_i)\in\mathbb{R}^2$, and the differentiation orders $\alpha_1<\alpha_2<\ldots<\alpha_{m_A},\beta_0<\beta_1<\ldots<\beta_{m_B}$ are allowed to be non-integer positive numbers. State space representation was extended by [19] to commensurate fractional systems, where all the differentiation orders are multiple integers of α. The extension was done by allowing the differentiation order of the state vector to be any commensurate order $\alpha\in\mathbb{R}^{+*}$. The fractional state space representation is presented in a MIMO case as:

$$\mathcal{D}^{\alpha}\mathbf{x}(t)=A\mathbf{x}(t)+B\mathbf{u}(t), \quad (1)$$

$$\mathbf{y}(t)=C\mathbf{x}(t)+D\mathbf{u}(t) \quad (2)$$

where $\mathbf{x}\in\mathbb{R}^n$ is the state vector, $\mathbf{u}\in\mathbb{R}^m$ the input vector, $\mathbf{y}\in\mathbb{R}^p$ the output vector, $A\in\mathbb{R}^{n\times n}$, $B\in\mathbb{R}^{n\times m}$, $C\in\mathbb{R}^{p\times n}$, $D\in\mathbb{R}^{p\times m}$ are constant matrices. Here, zero initial conditions are considered: $\mathbf{x}(t)=0$ for $t\leq 0$. Matignon [20] proved that the fractional system (1)-(2) is stable if:

$$0<\alpha<2 \quad \text{and} \quad |\arg(\lambda_k)|>\alpha\frac{\pi}{2} \quad \forall k=1,\ldots,n$$

where λ_k is the k^{th}-eigenvalue of A and $-\pi<\arg(\lambda_k)\leq\pi$.

The conversion of (1)-(2) to the MIMO transfer function form is obtained as for the rational systems by:

$$G(s)=C(s^{\alpha}I-A)^{-1}B+D$$

where s is the Laplace variable.

In the following, the pair (A, B) is assumed to be reachable and the pair (C, A) is assumed to be observable. The controllability and the observability conditions of a state space representation of a commensurate fractional system are the same as for rational systems [19].

One of the main difficulties with fractional models is the time-domain simulation. This problem has been extensively studied and an overview of the principal methods can be found in [21]. The most commonly used approximation of fractional operators is the recursive distribution of zeros and poles, proposed in [22], which approximates the frequency behavior of s^{α} in the frequency range $[\omega_A,\omega_B]$. Nevertheless, this approximation has null asymptotic behaviors at low and high frequencies, which can introduce a static error between the fractional model and its approximation. To avoid this drawback, Trigeassou *et al.* [5] suggested to use the conventional integrator outside the frequency range $[\omega_A,\omega_B]$:

$$s^{-\alpha}_{[\omega_A,\omega_B]}=\frac{G_\alpha}{s}\prod_{k=1}^{N_c}\frac{1+s/\omega'_k}{1+s/\omega_k} \quad (3)$$

where:

- N_c is the number of cells (directly related to the quality of the approximation),
- G_α is fixed so that $s^{-\alpha}$ has the same gain as $s^{-\alpha}_{[\omega_A,\omega_B]}$ in the middle of the interval $[\omega_A,\omega_B]$,
- ω'_k and ω_k are respectively zeros and poles recursively distributed in the frequency range $[\omega_b,\omega_h]=[\sigma^{-1}\omega_A,\sigma\omega_B]$ where σ is generally set to 10 to minimize border effects. They are defined by the following relations:

$$\omega'_k=\gamma\omega_k, \quad \omega_{k+1}=\eta\omega'_k, \quad \alpha=1-\frac{\log\gamma}{\log\gamma\eta}.$$

This approximation is used to simulate the fractional systems presented in this paper (section 5) with the parameters: $N_c=20$, $\omega_A=10^{-5}$ and $\omega_B=10^5$.

3 SUBSPACE ALGORITHMS FOR FRACTIONAL STATE-SPACE IDENTIFICATION

Consider the linear continuous-time fractional state-space representation (1)-(2) corrupted by additive noise:

$$\mathcal{D}^{\alpha}\mathbf{x}(t) = A\mathbf{x}(t) + B\mathbf{u}(t) + \mathbf{v}(t), \quad (4)$$
$$\mathbf{y}(t) = C\mathbf{x}(t) + D\mathbf{u}(t) + \mathbf{w}(t) \quad (5)$$

where $\mathbf{v} \in \mathbb{R}^n$ and $\mathbf{w} \in \mathbb{R}^p$ are zero-mean processes. Under some mild conditions on $\mathbf{v}$ and $\mathbf{v}$ (uniform spectrum, uncorrelation) [13], the state-space representation (4)-(5) can be replaced by the innovations model:

$$\mathcal{D}^{\alpha}\mathbf{x}(t) = A\mathbf{x}(t) + B\mathbf{u}(t) + K\mathbf{e}(t), \quad (6)$$
$$\mathbf{y}(t) = C\mathbf{x}(t) + D\mathbf{u}(t) + \mathbf{e}(t). \quad (7)$$

The problem in this section is to estimate the system matrices A, B, C, D from sampled input-output data[1] $\{\mathbf{u}_k\}_{k=0}^{N-1}$ and $\{\mathbf{y}_k\}_{k=0}^{N-1}$. The commensurate order α is assumed to be known. The case where α is unknown is discussed in section 4.

To introduce the difficulty of the continuous-time fractional state-space model identification, let us consider firstly the deterministic case ($\mathbf{e}(t) = \mathbf{0}$). Then, by computing the successive α-order fractional derivatives of (7) and by substitution, the following extended linear model is obtained:

$$\bar{\mathbf{y}}(t) = \Gamma_i^* \, \mathbf{x}(t) + \Phi_i^* \, \bar{\mathbf{u}}(t) \quad (8)$$

with input and output variables:

$$\bar{\mathbf{u}}(t) = [\mathbf{u}(t)^T \quad \mathcal{D}^{\alpha}\mathbf{u}(t)^T \quad \dots \quad \mathcal{D}^{i\alpha}\mathbf{u}(t)^T]^T$$
$$\bar{\mathbf{y}}(t) = [\mathbf{y}(t)^T \quad \mathcal{D}^{\alpha}\mathbf{y}(t)^T \quad \dots \quad \mathcal{D}^{i\alpha}\mathbf{y}(t)^T]^T$$

and

$$\Gamma_i^* = \begin{bmatrix} C \\ CA \\ \vdots \\ CA^{i-1} \end{bmatrix} \in \mathbb{R}^{ip \times n}, \; \Phi_i^* = \begin{bmatrix} D & 0 & \cdots & 0 \\ CB & D & \ddots & \vdots \\ \vdots & \ddots & \ddots & 0 \\ CA^{i-2}B & \cdots & CB & D \end{bmatrix} \in \mathbb{R}^{ip \times im}.$$

The structure of (8) is the same than the extended linear model used in classical discrete-time subspace identification methods [18]. Unfortunately, (8) contains the successive α-order fractional derivatives of the input-ouput data which are not measured in most practical cases and which are difficult to estimate particularly in a noisy framework [23].

To avoid this difficulty, the following operator (fractional low-pass filter) is introduced:

$$\Lambda(s) = \frac{1}{1 + \left(\frac{s}{\omega_f}\right)^{\alpha}} = \frac{1}{1 + \tau s^{\alpha}} \text{ with } \tau = (1/\omega_f)^{\alpha}. \quad (9)$$

Let us consider the Laplace transform of (6)-(7):

$$s^{\alpha}X(s) = AX(s) + BU(s) + KE(s) \quad (10)$$
$$Y(s) = CX(s) + DU(s) + E(s). \quad (11)$$

Then, (10) can be expressed as:

$$\begin{aligned} X(s) &= (I + \tau A)[\Lambda(s)X(s)] + \tau B[\Lambda(s)U(s)] + \tau K[\Lambda(s)E(s)] \\ &= A_\lambda[\Lambda(s)X(s)] + B_\lambda[\Lambda(s)U(s)] + K_\lambda[\Lambda(s)E(s)] \end{aligned}$$

with $A_\lambda = I + \tau A$, $B_\lambda = \tau B$ and $K_\lambda = \tau K$. Application of the inverse Laplace transform leads to the following system of linear equations:

$$\mathbf{x}(t) = A_\lambda[\lambda\mathbf{x}(t)] + B_\lambda[\lambda\mathbf{u}(t)] + K_\lambda[\lambda\mathbf{e}(t)] \quad (12)$$
$$\mathbf{y}(t) = C\mathbf{x}(t) + D\mathbf{u}(t) + \mathbf{e}(t) \quad (13)$$

where $\lambda\mathbf{x}(t)$, $\lambda\mathbf{u}(t)$ and $\lambda\mathbf{e}(t)$ correspond to the states, the inputs and the noise prefiltered by Λ in (9). Then, from (13), it is found by recursion that:

$$\begin{aligned} \mathbf{y}(t) &= C\mathbf{x}(t) + D\mathbf{u}(t) + \mathbf{e}(t) \\ &= CA_\lambda[\lambda\mathbf{x}(t)] + CB_\lambda[\lambda\mathbf{u}(t)] + D\mathbf{u}(t) + CK_\lambda[\lambda\mathbf{e}(t)] + \mathbf{e}(t) \\ &\quad \vdots \\ &= CA_\lambda^k[\lambda^k\mathbf{x}(t)] + \sum_{j=1}^{k} CA_\lambda^{k-j}B_\lambda[\lambda^{k-j+1}\mathbf{u}(t)] + D\mathbf{u}(t) \\ &\quad + \sum_{j=1}^{k} CA_\lambda^{k-j}K_\lambda[\lambda^{k-j+1}\mathbf{e}(t)] + \mathbf{e}(t) \end{aligned}$$

for $k \in \mathbb{N}^*$, where $\lambda^k\mathbf{x}(t)$ denotes the signals obtained from $\mathbf{x}(t)$ by filtering through a series of k low-pass filters Λ. In the same

[1] The discrete-time variables are denoted by x_k and correspond to the time sampling with a constant sampling period T_s of the continuous-time variable $x(t)$: $x_k = x(kT_s)$.

way, it is found for $l \in \mathbb{N}^*$:

$$\begin{aligned}
\lambda^l \mathbf{y}(t) &= C[\lambda^l \mathbf{x}(t)] + D[\lambda^l \mathbf{u}(t)] + [\lambda^l \mathbf{e}(t)] \\
&= CA_\lambda[\lambda^{l+1}\mathbf{x}(t)] + CB_\lambda[\lambda^{l+1}\mathbf{u}(t)] + D[\lambda^l \mathbf{u}(t)] \\
&\quad + CK_\lambda[\lambda^{l+1}\mathbf{e}(t)] + [\lambda^l \mathbf{e}(t)] \\
&\quad \vdots \\
&= CA_\lambda^{k-l}[\lambda^k \mathbf{x}(t)] + \sum_{j=1}^{k-l} CA_\lambda^{k-j-l} B_\lambda[\lambda^{k-j+1}\mathbf{u}(t)] \\
&\quad + D[\lambda^l \mathbf{u}(t)] + \sum_{j=1}^{k-l} CA_\lambda^{k-j-l} K_\lambda[\lambda^{k-j+1}\mathbf{e}(t)] + [\lambda^l \mathbf{e}(t)]
\end{aligned}$$

with $k \geq l$. As a consequence, the input-output data can be formulated as the following extended linear model (with no time derivatives of the data):

$$\mathcal{Y}(t) = \Gamma_i \, \mathcal{X}(t) + \Phi_i \, \mathcal{U}(t) + \Psi_i \mathcal{E}(t) \tag{14}$$

with state, input-output and noise variables: $\mathcal{X}(t) = \lambda^{i-1}\mathbf{x}(t)$

$$\mathcal{Y}(t) = \begin{bmatrix} \lambda^{i-1}\mathbf{y}(t) \\ \lambda^{i-2}\mathbf{y}(t) \\ \vdots \\ \lambda^1 \mathbf{y}(t) \\ \mathbf{y}(t) \end{bmatrix}, \; \mathcal{U}(t) = \begin{bmatrix} \lambda^{i-1}\mathbf{u}(t) \\ \lambda^{i-2}\mathbf{u}(t) \\ \vdots \\ \lambda^1 \mathbf{u}(t) \\ \mathbf{u}(t) \end{bmatrix}, \; \mathcal{E}(t) = \begin{bmatrix} \lambda^{i-1}\mathbf{e}(t) \\ \lambda^{i-2}\mathbf{e}(t) \\ \vdots \\ \lambda^1 \mathbf{e}(t) \\ \mathbf{e}(t) \end{bmatrix}$$

and:

$$\Gamma_i = \begin{bmatrix} C \\ CA_\lambda \\ \vdots \\ CA_\lambda^{i-1} \end{bmatrix}, \; \Phi_i = \begin{bmatrix} D & 0 & \cdots & 0 \\ CB_\lambda & D & \ddots & \vdots \\ \vdots & \ddots & \ddots & 0 \\ CA_\lambda^{i-2}B_\lambda & \cdots & CB_\lambda & D \end{bmatrix},$$

$$\Psi_i = \begin{bmatrix} I & 0 & \cdots & 0 \\ CK_\lambda & I & \ddots & \vdots \\ \vdots & \ddots & \ddots & 0 \\ CA_\lambda^{i-2}K_\lambda & \cdots & CK_\lambda & I \end{bmatrix}$$

where $\Gamma_i \in \mathbb{R}^{ip \times n}$ is the extended observability matrix and $\Phi_i \in \mathbb{R}^{ip \times im}$, $\Psi_i \in \mathbb{R}^{ip \times im}$ are block Toeplitz matrices. Now, from N available input-output samples observed at discrete times $t_k = kT_s$ for $k = 0, \ldots, N-1$, the extended linear model (14) can be rewritten as:

$$\mathcal{Y}_N = \Gamma_i \, \mathcal{X}_N + \Phi_i \, \mathcal{U}_N + \Psi_i \mathcal{E}_N \tag{15}$$

where

$$\mathcal{U}_N = \begin{bmatrix} [\lambda^{i-1}\mathbf{u}]_0 & [\lambda^{i-1}\mathbf{u}]_1 & \cdots & [\lambda^{i-1}\mathbf{u}]_{N-1} \\ [\lambda^{i-2}\mathbf{u}]_0 & [\lambda^{i-2}\mathbf{u}]_1 & \cdots & [\lambda^{i-2}\mathbf{u}]_{N-1} \\ \vdots & \vdots & & \vdots \\ [\lambda\mathbf{u}]_0 & [\lambda\mathbf{u}]_1 & \cdots & [\lambda\mathbf{u}]_{N-1} \\ \mathbf{u}_0 & \mathbf{u}_1 & \cdots & \mathbf{u}_{N-1} \end{bmatrix} \in \mathbb{R}^{mi \times N}$$

and $[\lambda^j \mathbf{u}]_k = \lambda^j \mathbf{u}(t_k)$ denotes the sampled filtered data. The matrices $\mathcal{Y}_N \in \mathbb{R}^{pi \times N}$, $\mathcal{X}_N \in \mathbb{R}^{n \times N}$ and $\mathcal{E}_N \in \mathbb{R}^{mi \times N}$ are constructed in a similar way. The formulation given in (15) enables to use subspace identification algorithms as in their original non-factional discrete-time version. The difference is the addition of a step in which the data are filtered (what is a classical step in continuous-time identification [23]). This lowpass filtering induces the tuning of an additional parameter ω_f whose the sensibility has been studied in [24].

3.1 Deterministic framework : MOESP algorithm

First, let us start by using the most popular subspace identification method called MOESP (MIMO output-error state space) algorithm [18, 25]. This is a deterministic approach based on the properties of the noiseless version of (15):

$$\mathcal{Y}_N = \Gamma_i \, \mathcal{X}_N + \Phi_i \, \mathcal{U}_N. \tag{16}$$

The principle of this algorithm is as follows:

1. Compute the LQ decomposition of the data matrix:

$$\begin{bmatrix} \mathcal{U}_N \\ \mathcal{Y}_N \end{bmatrix} = \begin{bmatrix} L_{11} & 0 \\ L_{21} & L_{22} \end{bmatrix} \begin{bmatrix} Q_1^T \\ Q_2^T \end{bmatrix} \tag{17}$$

   where $L_{11} \in \mathbb{R}^{im \times im}$, $L_{21} \in \mathbb{R}^{ip \times im}$, $L_{22} \in \mathbb{R}^{ip \times ip}$ with L_{11}, L_{22} lower triangular, and $Q_1 \in \mathbb{R}^{N \times im}$, $Q_2 \in \mathbb{R}^{N \times ip}$ are orthogonal.
2. Compute the singular value decomposition (SVD) of the L_{22} matrix approximating the column space of Γ_i:

$$L_{22} = \begin{bmatrix} U_1 \; U_2 \end{bmatrix} \begin{bmatrix} \Sigma_1 & 0 \\ 0 & 0 \end{bmatrix} \begin{bmatrix} V_1^T \\ V_2^T \end{bmatrix} \tag{18}$$

   where $U_1 \in \mathbb{R}^{ip \times n}$, $U_2 \in \mathbb{R}^{ip \times (ip-n)}$ and $\Sigma_1 \in \mathbb{R}^{n \times n}$. The state order n can be estimated from the SVD since $n = \dim \Sigma_1$ in the noiseless case.
3. Estimate the extended observability matrix: $\hat{\Gamma}_i = U_1 \Sigma_1^{1/2}$.
4. Estimate the C matrix: $\hat{C} = \hat{\Gamma}_i(1:p, 1:n)$.

5. Estimate A_λ by solving the linear equation:

$$\hat{\Gamma}_i\big(1:p(i-1),1:n\big)\,A_\lambda = \hat{\Gamma}_i\big(p+1:ip,1:n\big). \qquad (19)$$

6. Estimate the B_λ and D matrices. For that purpose, it can be shown that:

$$U_2^T\Psi_i = U_2^T L_{21}L_{11}^{-1} \qquad (20)$$

which is a linear equation with respect to B_λ and D. Define:

$$U_2^T \triangleq \begin{bmatrix}\mathcal{L}_1 & \mathcal{L}_2 & \cdots & \mathcal{L}_i\end{bmatrix} \qquad (21)$$
$$U_2^T L_{21}L_{11}^{-1} \triangleq \begin{bmatrix}\mathcal{M}_1 & \mathcal{M}_2 & \cdots & \mathcal{M}_i\end{bmatrix} \qquad (22)$$

with $\mathcal{L}_k \in \mathbb{R}^{(ip-n)\times p}$ and $\mathcal{M}_k \in \mathbb{R}^{(ip-n)\times m}$ for $k = 1,\ldots,i$. Thus, from (20):

$$\begin{aligned}
\mathcal{L}_1 D + \mathcal{L}_2\hat{C}D + \cdots + \mathcal{L}_i\hat{C}\hat{A}_\lambda^{i-2}B_\lambda &= \mathcal{M}_1\\
\mathcal{L}_2 D + \mathcal{L}_3\hat{C}D + \cdots + \mathcal{L}_i\hat{C}\hat{A}_\lambda^{i-3}B_\lambda &= \mathcal{M}_3\\
&\vdots\\
\mathcal{L}_{i-1}D + \mathcal{L}_i\hat{C}D &= \mathcal{M}_{i-1}\\
\mathcal{L}_i D &= \mathcal{M}_i.
\end{aligned}$$

Define $\bar{\mathcal{L}}_k = [\mathcal{L}_k \ \ldots \ \mathcal{L}_i] \in \mathbb{R}^{(ip-n)\times(i+1-k)p}$, $k = 2,\ldots,i$, and get the following overdetermined system of linear equations:

$$\begin{bmatrix}\mathcal{L}_1 & \bar{\mathcal{L}}_2\hat{\Gamma}_{i-1}\\ \mathcal{L}_2 & \bar{\mathcal{L}}_3\hat{\Gamma}_{i-2}\\ \vdots & \vdots\\ \mathcal{L}_{i-1} & \bar{\mathcal{L}}_i\hat{\Gamma}_1\\ \mathcal{L}_i & 0\end{bmatrix}\begin{bmatrix}D\\ B_\lambda\end{bmatrix} = \begin{bmatrix}\mathcal{M}_1\\ \mathcal{M}_2\\ \vdots\\ \mathcal{M}_{i-1}\\ \mathcal{M}_i\end{bmatrix} \qquad (23)$$

where the block coefficient matrix in the left-hand side is $i(ip-n)\times(p+n)$-dimensional. Estimates of B_λ and D are obtained by finding the least-squares solution of (23).

The matrices of the fractional continuous-time state-space representation (10)-(11) are then deduced as follows: $\hat{A} = \frac{1}{\tau}(\hat{A}_\lambda - I)$, $\hat{B} = \frac{1}{\tau}\hat{B}_\lambda$. The $\hat{C}$ and $\hat{D}$ matrices do not change.

This method is consistent in its discrete-time version if the output noise ($\mathbf{w}$) is white and if there is no process noise ($\mathbf{v} = 0$). In our framework, the filtering of the input-output data calls the consistency into question.

3.2 Stochastic framework: PO-MOESP algorithm

In a stochastic framework, instrumental variables can be used to remove the noise effect. The most popular method in this context is the PO-MOESP (Past Output MIMO Output-Error State Space) algorithm [25, 26]. First, the input and output data and the noise matrices are partitioned into two parts:

$$\mathcal{U}_N = \begin{bmatrix}\mathcal{U}_p\\ \mathcal{U}_f\end{bmatrix},\ \mathcal{Y}_N = \begin{bmatrix}\mathcal{Y}_p\\ \mathcal{Y}_f\end{bmatrix},\ \mathcal{E}_N = \begin{bmatrix}\mathcal{E}_p\\ \mathcal{E}_f\end{bmatrix}. \qquad (24)$$

The number of block rows in $\mathcal{U}_p$, $\mathcal{Y}_p$ and $\mathcal{E}_p$ is denoted by β. The number of block rows in $\mathcal{U}_f$, $\mathcal{Y}_f$ and $\mathcal{E}_f$ is then $\gamma = i - \beta$. These numbers can be chosen arbitrary, but it is generally preferred to set $\beta = \gamma$. By considering only the second part of these matrices, (15) becomes:

$$\mathcal{Y}_f = \Gamma_\gamma X_f + \Phi_\gamma \mathcal{U}_f + \Psi_\gamma\mathcal{E}_f. \qquad (25)$$

The instrumental variable introduced to remove the effects of the noise is $\mathcal{Z} = [\mathcal{U}_p^T\ \mathcal{Y}_p^T]^T$. Hence, the principle of the PO-MOESP algorithm is as follows:

1. Compute the LQ decomposition of the data matrix:

$$\begin{bmatrix}\mathcal{U}_f\\ \mathcal{U}_p\\ \mathcal{Y}_p\\ \mathcal{Y}_f\end{bmatrix} = \begin{bmatrix}L_{11} & 0 & 0 & 0\\ L_{21} & L_{22} & 0 & 0\\ L_{31} & L_{32} & L_{33} & 0\\ L_{41} & L_{42} & L_{43} & L_{44}\end{bmatrix}\begin{bmatrix}Q_1^T\\ Q_2^T\\ Q_3^T\\ Q_4^T\end{bmatrix} \qquad (26)$$

where all the matrices L_{jj} are lower triangular and all the matrices Q_j are orthogonal (for $j = 1,2,3,4$).

2. Compute the SVD of $[L_{42}\ L_{43}]$ which approximates the column space of Γ_γ:

$$\begin{bmatrix}L_{42} & L_{43}\end{bmatrix} = \begin{bmatrix}U_1 & U_2\end{bmatrix}\begin{bmatrix}\Sigma_1 & 0\\ 0 & 0\end{bmatrix}\begin{bmatrix}V_1^T\\ V_2^T\end{bmatrix} \qquad (27)$$

where $U_1 \in \mathbb{R}^{ip\times n}$, $U_2 \in \mathbb{R}^{ip\times(ip-n)}$ and $\Sigma_1 \in \mathbb{R}^{n\times n}$. As for the MOESP algorithm, the state-space order n can be estimated by calculating the number of significant singular values of $\begin{bmatrix}L_{42} & L_{43}\end{bmatrix}$.

The following steps 3, 4, 5 and 6 are the same as for the MOESP algorithm.

4 FRACTIONAL ORDER ESTIMATION

In this section, we assume that the fractional derivative order $\alpha \in (0,2)$ is unknown and has to be estimated by minimizing a

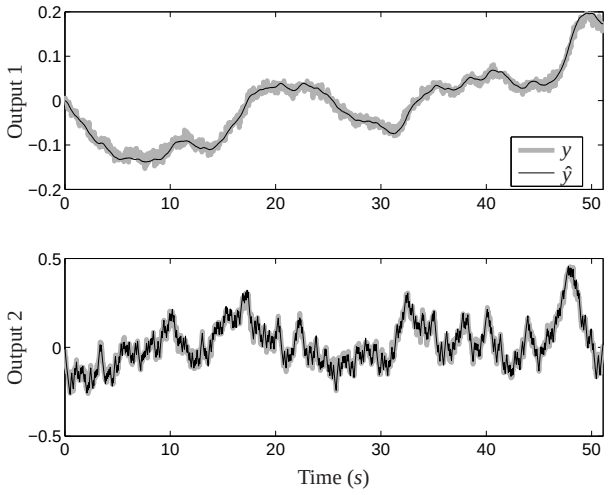

Figure 1. OUTPUT DATA $\mathbf{y}$ AND OUTPUT OF THE ESTIMATED MODEL $\hat{\mathbf{y}}$ WITH MOESP (SNR=20 dB, $i = 8$ AND $\omega_f = 6$).

quadratic criterion:

$$\hat{\alpha} = \arg \min_{\alpha \in (0,2)} \frac{1}{2} \|\hat{\mathbf{y}}_c(\alpha) - \mathbf{y}_c\|_2^2, \tag{28}$$

where $\mathbf{y}_c$ is the vector (of length pN) obtained by concatenating the p system outputs and $\hat{\mathbf{y}}_c(\alpha)$ is the vector obtained by concatenating the p outputs of the state-space representation estimated with one of the subspace methods (MOESP or PO-MOESP) for a given α. The value of α in (28) is obtained by a nonlinear optimization technique. The iterative algorithm used is based on a subspace trust-region method and on the interior-reflective Newton method described in [27]. Consequently, the proposed subspace algorithm is executed at each iteration of the optimization technique. The number of state variables n is assumed to be known. However, it may be estimated by using order estimation criteria presented in [28] .

5 SIMULATION EXAMPLES

The algorithms are applied to input-output data of length $N = 1023$ generated by simulating the linear system (1)-(2) with $\alpha = 0.9$,

$$A = \begin{bmatrix} 0 & -0.1 \\ 1 & -0.2 \end{bmatrix}, B = \begin{bmatrix} 1 \\ 0 \end{bmatrix}, C = \begin{bmatrix} 0 & 0.1 \\ 0.5 & -0.1 \end{bmatrix}, D = \begin{bmatrix} 0 \\ 0 \end{bmatrix},$$

and zero initial conditions ($\mathbf{x}(t) = 0$ for $t \leq 0$). The input signal is a pseudo-random binary sequence (PRBS) with maximum length. The sampling period is $T_s = 0.05s$. The outputs (Fig. 1) are corrupted by white noise with a signal-to-noise ratio (SNR) of 20 dB. The influence of the method parameters (the number of block rows i and the filter frequency ω_f) has been studied in [24]. It was shown that ω_f can be chosen in a suitable range over one decade, between 1 and 10 and that the choice of i influences more the results: acceptable results are obtained starting from $i = 6$. For this example, the algorithm parameters are fixed to $i = 8$ and $\omega_f = 6$.

5.1 Using the MOESP algorithm

The estimation results with the MOESP algorithm are:

$$\hat{\alpha} = 0.8894,$$
$$\hat{A} = \begin{bmatrix} 0 & -0.1008 \\ 1 & -0.1757 \end{bmatrix}, \hat{B} = \begin{bmatrix} 1 \\ 0 \end{bmatrix},$$
$$\hat{C} = \begin{bmatrix} 0.0012 & 0.1012 \\ 0.4997 & -0.0923 \end{bmatrix}, \hat{D} = \begin{bmatrix} 1.3782\,10^{-3} \\ -0.6763\,10^{-3} \end{bmatrix}.$$

The normalized prediction error norm $\|\hat{y} - y\|_2 / \|y\|_2$ equals 0.1050 (-19.57 dB) for the first output and 0.1008 (-19.93 dB) for the second one.

To analyze the statistical properties of the estimator, three Monte Carlo simulations are carried out for SNR of 20, 15 and 10 dB. Each simulation is done with 500 runs with different realizations of noise. The means of the normalized error norms, obtained with $i = 8$ and $\omega_f = 6$, are given in Tab. 1. Figure 2 shows the estimated poles. The normalized mean squared error (MSE) of the poles are indicated in Tab. 2. It can be seen that the pole estimator is biased. Moreover, as shown in the histograms of the estimated order α in Fig. 3, the order estimate is also biased, and the bias increases with the noise level. These biases are obviously introduced by the MOESP algorithm. Indeed, in order to guarantee the consistency of the estimates using this algorithm, the input must satisfy the persistent excitation condition (verified with a PRBS for example) and the output noise have to be white [29]. In fact, the latter condition is not satisfied because of the data filtering.

5.2 Using the PO-MOESP algorithm

The PO-MOESP algorithm applied to the same input-output data gives the following estimates:

$$\hat{\alpha} = 0.9021,$$
$$\hat{A} = \begin{bmatrix} 0 & -0.0999 \\ 1 & -0.2072 \end{bmatrix}, \hat{B} = \begin{bmatrix} 1 \\ 0 \end{bmatrix},$$
$$\hat{C} = \begin{bmatrix} 0.0006 & 0.1007 \\ 0.5008 & -0.1020 \end{bmatrix}, \hat{D} = \begin{bmatrix} 0.4564\,10^{-3} \\ 0.0491\,10^{-3} \end{bmatrix}.$$

Table 1. MEANS OF THE NORMALIZED ERROR NORMS.

	output	SNR=20 dB	SNR=15 dB	SNR=10 dB
MOESP	1	0.1026	0.1834	0.3327
		(−19.78 dB)	(−14.73 dB)	(−9.56 dB)
	2	0.1005	0.1797	0.3282
		(−19.95 dB)	(−14.91 dB)	(−9.68 dB)
PO-MOESP	1	0.1000	0.1760	0.3038
		(−20.00 dB)	(−15.09 dB)	(−10.35 dB)
	2	0.0991	0.1745	0.3010
		(−20.08 dB)	(−15.16 dB)	(−10.43 dB)

Table 2. NORMALIZED MSE OF THE POLES.

SNR	MOESP	PO-MOESP
20 dB	$(-0.4952 \pm i\,0.8875).10^{-4}$	$(0.4661 \pm i\,0.5006).10^{-4}$
15 dB	$(-0.2530 \pm i\,0.6315).10^{-3}$	$(0.1634 \pm i\,0.1976).10^{-3}$
10 dB	$(-0.1208 \pm i\,0.5740).10^{-2}$	$(0.4651 \pm i\,0.7347).10^{-3}$

The normalized prediction error norm equals 0.0983 (−20.15 dB) for the first output and 0.0989 (−20.09 dB) for the second one. So the results are improved with the PO-MOESP algorithm.

The same Monte Carlo simulations are performed as previously. Table 1 gives the means of the normalized error norms. Figure 4 shows the estimated poles. Their normalized MSE are indicated in Tab. 2. The estimates are unbiased but a slight increase of the variance is observed as compared to the results obtained with the MOESP algorithm. However, the normalized MSE is smaller, especially for a low SNR.

As shown in the histograms of the estimated order α in Fig. 5, the estimation is now unbiased. Moreover, the variance on the estimated parameter α is improved.

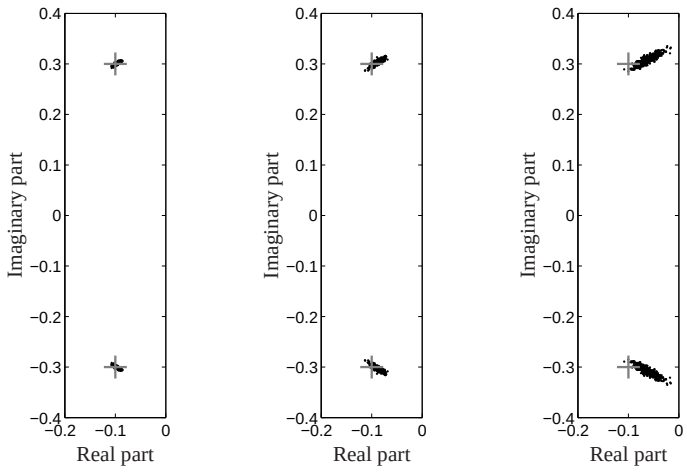

(a) SNR=20 dB (b) SNR=15 dB (c) SNR=10 dB

Figure 2. ESTIMATED POLES WITH MOESP, WHERE + DENOTES THE TRUE POLES.

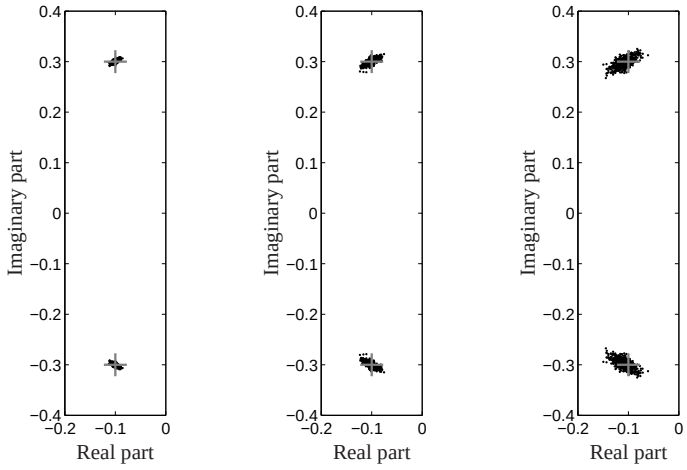

(a) SNR=20 dB (b) SNR=15 dB (c) SNR=10 dB

Figure 4. ESTIMATED POLES WITH PO-MOESP, WHERE + DENOTES THE TRUE POLES.

6 CONCLUSION

This paper focuses on the identification of continuous-time fractional state-space representation. Thanks to an adapted data filtering, we have shown that subspace-based algorithms can be used to estimate the state-space matrices. Results on the identification of a multivariable system with the well-known MOESP and PO-MOESP algorithms are given. The commensurate differentiation order is estimated by using nonlinear programming. Simulation examples have shown that the estimators are biased with the MOESP algorithm. However, the PO-MOESP algorithm eliminates this bias by using an instrumental variable. The limitation of this approach is that the design of the instruments requires an increased number of block rows i, i.e. an increase of the series of fractional low-pass filters $\Lambda(s)$, which leads to an excessive computational cost. So, a future work could be to consider another instruments to solve this problem.

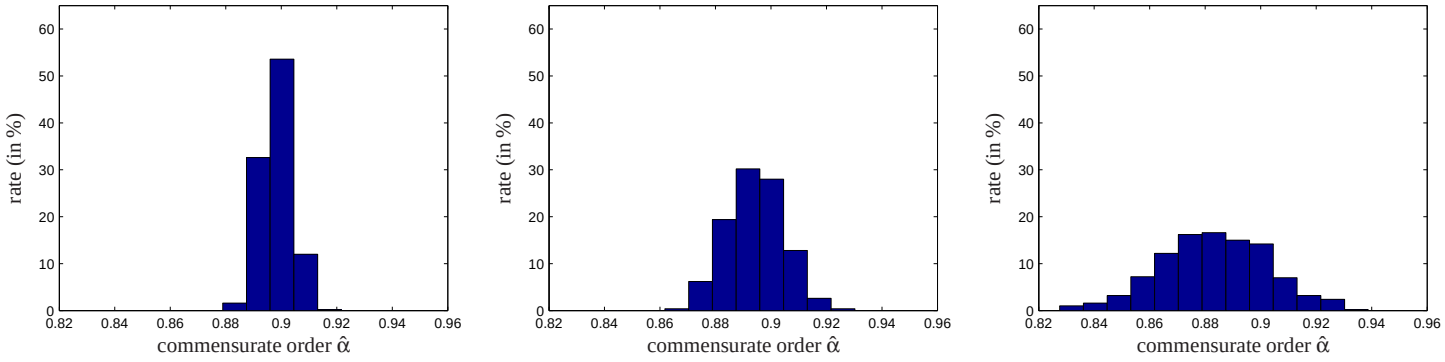

(a) SNR=20 dB (b) SNR=15 dB (c) SNR=10 dB

Figure 3. HISTOGRAMS OF THE ESTIMATED COMMENSURATE ORDER α WITH MOESP.

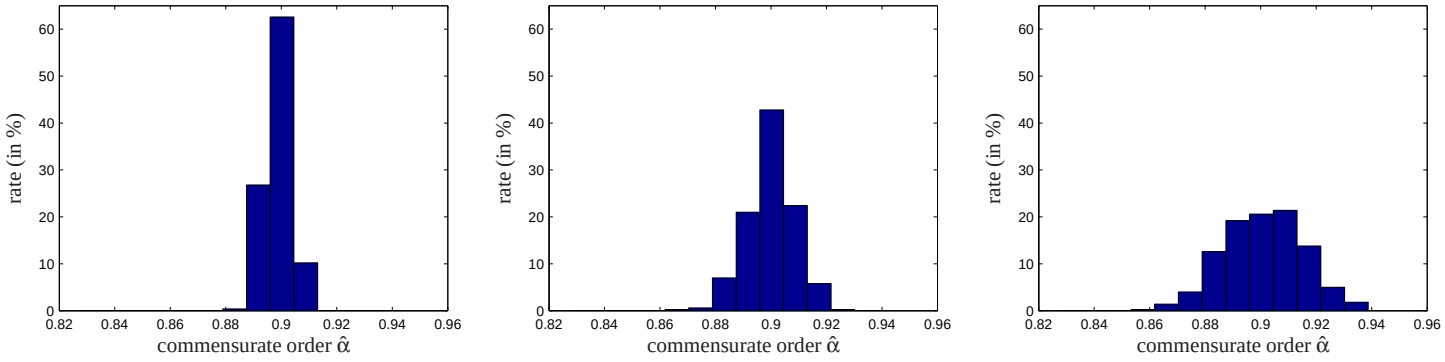

(a) SNR=20 dB (b) SNR=15 dB (c) SNR=10 dB

Figure 5. HISTOGRAMS OF THE ESTIMATED COMMENSURATE ORDER α WITH PO-MOESP.

REFERENCES

[1] Sabatier, J., Aoun, M., Oustaloup, A., Grégoire, G., Ragot, F., and Roy, P., 2006. "Fractional system identification for lead acid battery sate charge estimation". *Signal Processing*, **86**(10), pp. 2645–2657.

[2] Oldham, K. B., and Spanier, J., 1973. "Diffusive transport to planar, cylindrical and spherical electrodes". *Electroanal. Chem. Interfacial Electrochem.*, **41**, pp. 351–358.

[3] Battaglia, J.-L., Cois, O., Puigsegur, L., and Oustaloup, A., 2001. "Solving an inverse heat conduction problem using a non-integer identified model". *Int. J. of Heat and Mass Transfer*, **44**(14), pp. 2671–2680.

[4] Oustaloup, A., Le Lay, L., and Mathieu, B., 1996. "Identification of non integer order system in the time-domain". In IEEE-CESA'96, SMC IMACS Multiconference.

[5] Trigeassou, J.-C., Poinot, T., Lin, J., Oustaloup, A., and Levron, F., 1999. "Modeling and identification of a non integer order system". In Proc. of the European Control Conference.

[6] Cois, O., Oustaloup, A., Poinot, T., and Battaglia, J.-L., 2001. "Fractional state variabe filter for system identification by fractional model". In Proc. of the European Control Conference.

[7] Aoun, M., Malti, R., Levron, F., and Oustaloup, A., 2007. "Synthesis of fractional Laguerre basis for system approximation". *Automatica*, **43**(9), September, pp. 1640–1648.

[8] Malti, R., Victor, S., Oustaloup, A., and Garnier, H., 2008. "An optimal instrumental variable method for continuous-time fractional model identification". In Proc. of the 17th IFAC World congress.

[9] Malti, R., Victor, S., and Oustaloup, A., 2008. "Advances in system identification using fractional models". *Journal of Computational and Nonlinear Dynamics*, **3**(2), January.

[10] Poinot, T., and Trigeassou, J.-C., 2004. "Identification of fractional systems using an output-error technique". *Nonlinear Dynamics*, **38**(1-2), pp. 133–154.

[11] Haverkamp, B. R. J., Chou, C. T., Verhaegen, M., and Johansson, R., 1996. "Identification of continuous-time MIMO state space models from sampled data, in the presence of process and measurement noise". In Proc. of the

35th Conference on Decision and Control.
[12] Johansson, R., Verhaegen, M., and Chou, C. T., 1997. "Stochastic theory of continuous-time state-space identification". In Proc. of the 36th Conference on Decision and Control.
[13] Johansson, R., Verhaegen, M., and Chou, C. T., 1999. "Stochastic theory of continuous-time state-space identification". *IEEE Trans. Signal Processing*, **47**(1), pp. 41–51.
[14] Bastogne, T., Garnier, H., and Sibille, P., 2001. "A PMF-based subspace method for continuous-time model identification. Application to a multivariable winding process". *International Journal of Control*, **74**(2), pp. 118–132.
[15] Ohsumi, A., Kameyama, K., and Yamaguchi, K.-I., 2002. "Subspace identification for continuous-time stochastic systems via distribution-based approach". *Automatica*, **38**, pp. 63–79.
[16] Li, W., Raghavan, H., and Shah, S., 2003. "Subspace identification of continuous time models for process fault detection and isolation". *Journal of Process Control*, **13**, pp. 407–421.
[17] Mercère, G., Ouvrard, R., Gilson, M., and Garnier, H., 2007. "Subspace-based methods for continuous-time model identification of MIMO systems from filtered sampled data". In Proceedings of the European Control Conference.
[18] Katayama, T., 2005. *Subspace methods for system identification*. Springer.
[19] Matignon, D., and d'Andréa Novel, B., 1996. "Some results on controllability and observability of finite-dimensional fractional differential systems". In IEEE-CESA'96, SMC IMACS Multiconference, pp. 952–956.
[20] Matignon, D., 1998. "Stability properties for generalized fractional differential systems". In ESAIM : Proceedings, Fractional Differential Systems: Models, Methods and Applications, Vol. 5, pp. 145–158.
[21] Aoun, M., Malti, R., Levron, F., and Oustaloup, A., 2004. "Numerical simulations of fractional systems: an overview of existing methods and improvements". *Nonlinear Dynamics*, **38**, pp. 117–131.
[22] Oustaloup, A., 1995. *La dérivation non entière. Théorie, synthèse et applications*. Hermès, Paris.
[23] Garnier, H., and Wang, L., eds., 2008. *Identification of Continuous-Time Models from Sampled Data*. Springer.
[24] Thomassin, M., and Malti, R., 2009. "Subspace method for continuous-time fractional system identification". In Proc. of the 15th IFAC Symp. on System Identification (SYSID 2009).
[25] Viberg, M., 1995. "Subspace-based methods for the identification of linear time-invariant systems". *Automatica*, **31**(12), pp. 1835–1851.
[26] Verhaegen, M., 1994. "Identification of the deterministic part of MIMO state space models given in innovations form from input-output data". *Automatica*, **30**, pp. 61–74.
[27] Coleman, T. F., and Li, Y., 1996. "An interior, trust region approach for nonlinear minimization subject to bounds". *SIAM Journal on Optimization*, **6**, pp. 418–445.
[28] Bauer, D., 2001. "Order estimation for subspace methods". *Automatica*, **37**, pp. 1561–1573.
[29] Bauer, D., and Jansson, M., 2000. "Analysis of the asymptotic properties of the MOESP type of subspace algorithms". *Automatica*, **36**, pp. 497–509.